

MECHANISMS OF VIBRATION AND BVI NOISE REDUCTION BY
HIGHER HARMONIC CONTROL

BY

R. KUBE
B. v. d. WALL
K.-J. SCHULTZ

DEUTSCHE FORSCHUNGSANSTALT FÜR
LUFT- UND RAUMFAHRT E.V. (DLR)
D-38108 BRAUNSCHWEIG, GERMANY

TWENTIETH EUROPEAN ROTORCRAFT FORUM
OCTOBER 4 - 7, 1994 AMSTERDAM

Mechanisms of Vibration and BVI Noise Reduction by Higher Harmonic Control

R. Kube
B. v. d. Wall
K.-J. Schultz

Deutsche Forschungsanstalt für
Luft- und Raumfahrt e.V. (DLR)
D-38108 Braunschweig, Germany

Abstract

Besides a reduction of the vibrations Higher Harmonic Control (HHC) also allows a minimization of the Blade Vortex Interaction (BVI) noise. This has been demonstrated by means of wind tunnel tests which were conducted with the DLR rotor test rig in the German Dutch Wind Tunnel (DNW). The tests yielded a BVI noise reduction of up to 6 dB, unfortunately accompanied by an increased vibration level. The evaluation of the test data gave a first impression of the vibration and BVI noise reducing mechanisms in case of higher harmonic control. It was verified by numerical simulations providing informations about the blade vortex miss distance as well as the rotor dynamics and thus made it possible to determine the blade modes mainly contributing to a vibration and BVI noise suppression.

1. Introduction

Even in hover but especially in forward flight, rotary wing flow fields are much more complex than the ones of fixed wing aircrafts. The reason is, that the blades experience a periodically azimuthal variation of the velocity which, in addition, increases linearly with the rotor radius. This results in an asymmetric loading over the rotor disc and a strong tip vortex, both leading to a very difficile wake geometry.

Especially during landing approach, the rotor operates in this wake, thus generating a high vibration and noise level. Since both disturbances are very annoying, rotorcraft industries and research institutions have devoted a significant part of their activities to vibration and noise minimization in the past. Although progress has been made by applying passive means, like rotor isolation systems on the vibration side and blade tip geometry optimization on the noise side for example, further improvements are required. If, for example, landing at an inner-city vertiport is intended, the blade vortex interaction noise has to be diminished. This pulse-type noise is due to blade interaction with shed vortices of preceding blades and can be reduced by decreasing the blade lift and vortex strenght while increasing the blade/vortex miss distance at the blade vortex encounters.

These parameters can be affected by means of Higher Harmonic Control (HHC), a method which superimposes a higher harmonic blade pitch angle with low amplitude

to the conventional one. Originally developed for vibration minimization, HHC affects the aerodynamic forces acting on the rotor blades and therefore is able to reduce the BVI noise as well. This was demonstrated by a number of flight tests and wind tunnel experiments [1,2,3]. Those which were conducted with the DLR rotor test rig in the German Dutch Wind Tunnel yielded a BVI noise reduction of up to 6dB [4]. However, one unfavorable result of these tests was the correlation of the BVI noise and the vibration level. Both turned out to be counteracting which means, that a reduction of the BVI noise level is accompanied by an increased vibration level and vice versa. This result was very surprising because both disturbances originate from the same phenomena, the unsteady aerodynamic forces acting on the rotor blades. Therefore, a higher harmonic blade pitch angle leading to a minimum BVI noise level was expected to reduce the vibrations simultaneously.

Instead, the above mentioned counteracting correlation between BVI noise and vibration level occurred as long as a higher harmonic blade pitch angle consisting of one HHC frequency only was generated. However, if additional HHC frequencies were taken into account a reduction of the BVI noise accompanied by a nearly unaffected vibration level was possible [5].

In order to gain a physical understanding of these results, a detailed data evaluation was performed which showed, that the vibrations are clearly correlated to the flapping moment at the blade root and obviously are a result of the inertia forces associated with the blade motion. Therefore, a vibration suppression can only be achieved by reducing the blade flapping motion, thus minimizing the blade vortex miss distance and with that maximizing the BVI noise.

The validity of these assumptions was proofed by means of numerical simulations using a sophisticated rotor simulation model [6] and noise prediction code [7]. Both are introduced in the paper after the wind tunnel tests and the corresponding dynamic and acoustic results have been described. The importance of a blade flapping motion for a reduction of the BVI noise level will be demonstrated and one of the reasons for the counteracting correlation between vibrations and BVI noise will be specified.

2. Helicopter Vibrations and BVI Noise

The vibrations and noise emissions of a helicopter are known to be very intense during landing approach, where the rotor operates in its own wake. Both originate from the unsteady aerodynamic forces acting on the rotor blades which are due to reverse and radial flow, shock and stall effects, blade vortex interactions etc.. These phenomena are clearly associated with fixed rotor azimuth positions (fig. 1) and therefore let the aerodynamic blade forcing terms become of periodical type. The corresponding blade oscillations, occurring in flap and lead-lag directions as a result of the limited blade stiffness, cause additional inertia and elastic forces which, in combination with the aerodynamic forces, form the resultant blade loads (fig. 2). They consist exclusively of so called rotor harmonic (fig. 3) which cancel each other widely when the loads of the individual blades are superimposed in order to determine the corresponding forces acting on the fuselage [8]. The only remaining harmonics are integral multiples of the blade passage frequency

$$f_n = n \cdot b \cdot f_R$$

with

f_R the rotor rotational frequency,

b the number of blades

and

n an integral number.

From these harmonics, the lowest one is not only associated with the strongest amplitude but, furthermore, represents the most annoying part for human kind. It is known to be caused by blade loads of the frequencies $(b-1) \cdot f_R$, $b \cdot f_R$ and $(b+1) \cdot f_R$ [8], as is indicated in fig. 3 exemplarily for a four bladed rotor.

The BVI noise, however, is formed by the 6-th to 40-th blade passage frequency (fig. 4) and, therefore, represents a very high frequent disturbance. It is due to parallel blade vortex interactions at 60° rotor azimuth approximately with the vortex generated within the proximity of 120° (fig. 5). Passing close to the blade, the vortex changes the blade loading very rapidly, thus leading to a pulse-type noise emission which intensity is proportional to the inverse squared blade-vortex missdistance, the vortex strength and the blade lift at the blade-vortex encounters.

3. Higher Harmonic Control for Vibration and BVI Noise Reduction

Higher Harmonic Control is a technique which superposes a high-frequency blade pitch angle with, in general, low amplitude to the conventional one and, therefore, allows a suppression of the helicopter vibrations and BVI noise emissions at the source. By this superposition, the aerodynamic forcing terms and, consequently, the oscillations of the rotor blades can be affected. Both are coupled with each other, because the blade flapping degree of freedom influences directly the blade angle of attack, thus preventing that elastic, inertia and aerodynamic forces can be controlled independently. However, despite of this coupling a higher harmonic blade pitch angle allows a modification of the resultant blade loads and, with that, a minimization of the fuselage vibrations.

Besides this minimization of the vibrations, a modification of the blade loads by higher harmonic control also allows a reduction of the BVI noise level. If HHC amplitude and phase shift are for example adjusted in a way, that leads to an increased blade angle

of attack within a rotor azimuth interval around 60° and 120° respectively, the vortex strength and/or blade lift during interaction and, with that, the BVI noise emissions can be expected to be strengthened. However, this increase of the blade angle of attack also affects the blade-vortex missdistance by modifying both, the vortex trajectories [9] and the blade flapping oscillations [10]. Like the elastic, inertia and aerodynamic forces forming the blade loads and causing the vibrations in the fuselage finally, the BVI noise relevant parameters like blade-vortex missdistance, vortex strength and blade lift at the blade vortex encounters can also not be controlled independently. Although increasing the blade lift at the blade-vortex encounters, a higher harmonic blade pitch angle may therefore simultaneously enlarge the blade-vortex missdistance, thus reducing the BVI noise.

4. Wind Tunnel Tests

4.1 Test Setup

In order to verify the assumed vibration and BVI noise reducing potential of higher harmonic control, a wind tunnel experiment was performed in the DNW open jet configuration [11]. It was conducted with the DLR rotor test rig ROTEST (fig. 6) whichs major part is formed by the rotor balance. Consisting of an upper and lower plate connected by seven sensor systems (fig. 7), this balance measures both, the static as well as the dynamic forces and moments. On the upper plate three electro-hydraulic actuators are located which have a high cut-off frequency and therefore feature HHC capabilities, with an authority of up to 3° . The rotor, a mach-scaled model of the hingeless BO105 main rotor, is driven by a hydraulic motor and is equipped with strain gauges measuring the blade bending moments in flap, lead-lag and torsional direction.

For the wind tunnel experiments, the rotor test rig was installed in the DNW open jet test section which is known to be associated with a low background noise level as well as excellent anechoic properties and flow characteristics. Fig. 8 shows the DNW open jet configuration with the HHC test setup including a movable microphone array. This microphone array was used to register the noise emissions of the rotor and was mounted on a traversing system. It made it possible to measure the noise within a large plane below the rotor hub and, thus, allowed a determination of both, the achieved noise reduction and the changes in directivity pattern.

Microphone array and traversing system were covered with open cell foam in order to avoid rotor noise reflections. In combination with the sound absorptive lining of rotor test rig and DNW sting mechanism, this acoustical treatment of the in-flow microphone traverse made it possible to maintain the excellent anechoic properties of the DNW open jet test section, a prerequisite for high quality acoustic data.

4.2 Test Procedure and Test Matrix

In order to determine the effects of a higher harmonic blade pitch angle on the BVI noise radiation within the complete measurement plane below the rotor, the inflow microphone traverse had to be moved from -4m upstream to +4m the downstream the

rotor hub and back again for each rotor condition and HHC setting. In order to minimize the time required for this traverse movement, an "on-the-fly" data acquisition technique was applied. It employed a continuously moving microphone traverse with the data acquisition automatically activated at 17 pre-selected streamwise positions. Compared to a stop-and-go traversing procedure, this continuous microphone array movement made it possible to reduce the data acquisition time by a factor of five at twice the spatial resolution in flow direction. However, in order to approach stationary acoustic measurements, the traversing speed had to be set to a very low value, thus leading to a time period of 6 minutes for one traverse run approximately. Despite of the applied "on-the-fly" data acquisition technique, the acoustic measurements, therefore, were still very time consuming, thus allowing no systematic variation of all HHC parameters.

For that reason, the HHC amplitude was limited to 0.4°, 0.8° and 1.2° while the corresponding phase shift was varied in steps of 30° from 0° to 330°. This was done for a 3-, 4- and 5/rev blade pitch angle at a number of flight conditions, most of them representing a descent flight at different velocities and thrust coefficients (fig. 9). The nominal test condition was a simulated 1g-landing approach at an advance ration of 0.15 and a glide path angle of 6° corresponding to a wind tunnel velocity of 33 m/s and a corrected tip path plane angle of 5.3°.

4.3 Test Results

4.3.1 Vibration Reduction

Although in landing approach the vibrations are not the most intense ones [12], their reduction increases the flight comfort and, therefore, is highly appreciated. From previous investigations concentrating on forward flight conditions, these vibrations can be assumed to be due to inertia forces resulting from an excitation of the rotor blade's second flapping mode [10]. It has an eigenfrequency of $2.7 f_{\rho}$ and, therefore, is quite sensitive to 3/rev aerodynamic forces. Once excited by these forces, the flapping mode reacts with the same frequency, leading, for example, to strong 3/rev blade bending moments in flapping direction.

This is demonstrated in fig. 10 which shows the vibration relevant blade flapping moment's harmonics occurring during landing approach when higher harmonic control is not activated. The figure demonstrates the dominance of the 3/rev part, thus indicating that the second blade flapping mode is, in fact, strongly excited during landing approach, too. Like in forward flight, its reduction by means of a 3/rev blade pitch angle, for example, therefore leads to a minimization of the vibrations as can be seen from fig. 11 and 12. These figures show the 4/rev rotor forces and moments plotted versus 3/rev phase shift and make clear that for an HHC phase shift of 210° all dynamic rotor components reach simultaneously their absolute minimum. Consequently, this is also true for the vibration quality criterion

$$GF = F_x^2 + F_y^2 + F_z^2 + M_x^2 + M_y^2$$

with

F_x, F_y, F_z the 4/rev rotor forces,

and

M_x, M_y the 4/rev rotor moments

which, as can be seen from fig. 13 and 14, is clearly correlated with the 3/rev blade flap bending and obviously is reduced by eliminating the inertia forces caused by blade oscillations in flapwise direction.

4.3.2 BVI Noise Reduction

The effects of a higher harmonic blade pitch angle on the BVI noise can be demonstrated by means of sound pressure time histories. The ones shown in fig. 15 result from an observer location at maximum advancing side BVI and make clear that, in case without HHC, strong pulses occur, which are related to a blade-vortex interaction and which are nearly eliminated when higher harmonic control is enabled. Low frequency noise is seen increased in this case, however, this noise type is not very annoying for human kind. Therefore a so called mid-frequency noise level

$$L_{mid} = 10 \cdot \log_{10} \frac{\sum_{i=6}^{40} (a_i^2 + b_i^2)}{4 \cdot 10^{-10}}$$

with

a_i the real part of the Fourier coefficient corresponding to the i-th blade passage frequency

and

b_i the imaginary part of the Fourier coefficient corresponding to the i-th blade passage frequency

has been introduced, taking into account only the 6th to 40th blade passage frequency harmonic, i.e. the 24th to 160th rotor harmonic. The distribution of this measure within the plane of the movable microphones for the baseline and HHC case is shown in fig. 16 which makes clear, that the maximum BVI noise level occurring on the advancing side at roughly 90° rotor azimuth can be reduced by more than 5 dB

if a suited higher harmonic blade pitch angle is superposed to the conventional one.

4.3.3 Correlation of Vibrations and BVI Noise

Since vibrations and BVI Noise originate from the unsteady aerodynamic forces acting on the rotor blades, they were originally expected to be reduced simultaneously when higher harmonic control is applied. However, during the wind tunnel tests both disturbances turned out to be counteracting, as is demonstrated by fig. 17. It shows the averaged mid-frequency noise level of the complete measurement plane plotted versus 3/rev phase shift and, by comparison with fig. 14, demonstrates that the BVI noise minimum is clearly related to a vibration maximum.

Keeping in mind that the vibrations can be assumed to be due to inertia forces caused by blade oscillations, one prime candidate involved in vibration and BVI noise reduction is an increase of the blade-vortex missdistance. Provided it is due to an excitation of the second flapping mode, it would reduce the noise emissions of the rotor on the one hand but on the other hand would amplify the vibrations.

5. Theoretical Investigations

5.1 Rotor and Aeroacoustic Simulation Model

5.1.1 Blade Elastics

In order to procure additional informations of the mechanisms involved in vibration and BVI noise reduction by higher harmonic control, a computer code was used which describes the rotor dynamics in a way appropriate for HHC [6]. For that purpose up to three flapping, two lead-lag and one torsional mode is used to determine the blade motion in all three degrees of freedom. The mode shapes result from a finite element calculation and are represented by polynoms of 6th order. The modes to be taken into account for the simulation run can be selected interactively by the user thus allowing to investigate the contributions of individual modes to the simulation results.

5.1.2 Rotor Downwash

Besides the blade-mode combination, the type of downwash modelling can be chosen, too. One possibility is the Mangler-Squire method [13] which yields a non-uniform distribution of the induced velocity within the rotor disk and, therefore, represents the minimum requirement for simulations in combination with HHC.

An alternative to the Mangler model is a method following Beddoes [14]. It uses individual vortices with prescribed distorted geometry for the description of the downwash and therefore is better suited to represent effects like blade-vortex interaction, for example.

5.1.3 Profile Aerodynamics

For the calculation of profile lift, drag and moment an unsteady aerodynamic model

is used [15]. It represents not only the static behaviour perfectly but allows also periodic profile motions. Combining the Duhamel integral with the Wagner function [16] for harmonic oscillations of both the angle of attack and flap, the unsteady aerodynamic model describes the phase shift between angle of attack and angle of incidence analytically as a function of the angle of incidence's first and second derivative with respect to time, the mach number and the frequency of motion.

5.1.4 Aeroacoustic Simulation Model

The aeroacoustic simulation model is represented by the Ffowcs-Williams-Hawkings equation which represents the sound pressure for an instantaneous time at a certain observer position by three source integral terms radiating from the source location at an retarded time [7]. Whereas two of them account for thickness and loading noise, the third one is most effective in the transonic blade tip region and includes also effects like shock, for example.

For the numerical approach, the blade surface is subdivided into a number of source panels with individual characteristics at the retarded time. For each time step, the three source integral terms have to be determined for every panel, before all panel contributions are summed up with the correct time delays.

5.2 Simulation Procedure

For the simulations aiming on an investigation of the mechanisms involved in vibration and BVI noise reduction by HHC three flap, two lead-lag and one torsional mode taken into account. The rotor downwash was described by means of the method following Beddoes while profile lift, drag and moment were calculated using the unsteady aerodynamic model.

For each HHC setting a number of simulation steps had to be performed, in order to account for the tip path plane variation due to HHC inputs (fig. 18). For the first one, the induced velocities precalculated for a tip path plane perpendicular to the rotor shaft were used but with higher harmonic control activated. Based on these results, the induced velocities were adapted to the change in tip path plane orientation due to HHC inputs before the third and final rotor simulation run, yielding the fixed frame vibrations, the blade deflections and the blade loadings was conducted. The latter ones represented the input for the aeroacoustic simulation model calculating the BVI noise level distribution as well as the maximum and averaged value of the complete microphone plane.

5.3 Simulation Results

5.3.1 Vibration Reduction

A first result of the simulations conducted for the 6° landing approach flight condition is shown in fig. 19 which, by comparison with fig. 20 and 21, clarifies that the absolute vibration minimum at approximately 200° rotor azimuth clearly originates from a reduced excitation of both the first and second flapping mode. Due to its

eigenfrequency of $2.7f_R$, the second flapping mode is heavily affected by the 3/rev blade pitch angle, and therefore represents the prime contributor to the vibration level and its reduction by higher harmonic control.

5.3.2 Noise Reduction

The simulated effect of HHC on the blade vortex interaction noise is shown in fig. 23 which shows the BVI noise pattern within the microphone plane as it occurs in baseline case and in minimum noise case. The plot clarifies, that the simulated BVI noise level is overpredicted in general, however, the advancing and retreating side maximum can clearly be identified.

Like in wind tunnel, both can be reduced considerably by means of a 3/rev blade pitch angle, a result which is also demonstrated by the simulated microphone time history shown in fig. 22. As can be seen from fig. 24 and 25, this noise reduction is due to an increased blade-vortex missdistance at 45° rotor azimuth where the BVI noise relevant parallel blade vortex interactions occur. It is caused by a modified blade deflection in flapwise direction which mainly originates from an increased excitation of the second flapping mode. In combination with the finding that a vibration minimization requires a suppression of the first and second flapping mode's excitation, this result gives an explanation for the counteracting correlation between noise and vibrations in case of higher harmonic control.

6. Conclusions

Based on the results of a wind tunnel entry with the DLR rotor test rig in the German Dutch Wind Tunnel, the mechanisms of vibration and BVI noise reduction by higher harmonic control were investigated. For that purpose, the result of previous investigations, demonstrating that in forward flight the vibrations are due to the inertia forces caused by blade oscillations, was hypothetically extended to BVI flight conditions and then was validated by correlating the fixed frame vibrations with the bending moment at the blade root. Again it turned out that the 3/rev flapping moment has a relative high amplitude in baseline case and that its suppression by means of a higher harmonic blade pitch angle leads to a minimum of the vibrations.

However, this vibration suppression was accompanied by an increased BVI noise level whereas a reduction of the BVI noise led to a strong vibration amplification. The reason for this counteracting correlation was postulated to be due to the fact that the BVI noise level strongly depends on the blade-vortex missdistance which obviously is reduced by suppressing the 3/rev blade bending moment in order to minimize the fixed frame vibrations.

Within the scope of simulations this 3/rev blade bending moment was identified to be due to blade deflections mainly caused by a strong excitation of the second flapping mode. It has an eigenfrequency of $2.7f_R$ and therefore is quite sensitive to 3/rev aerodynamic forces. However, it is also very sensitive to 3/rev HHC inputs and therefore can very well be suppressed. As could be derived from the simulation

results, this suppression reduces not only the inertia forces due to blade oscillations but also the blade vortex missdistance, a finding which gives an explanation for the counteracting correlation of vibrations and BVI noise. It therefore seems to be quite confident, although in reality an additional effect from the modified wake geometry due to higher harmonic control can be expected. However, even if it is not the only mechanism involved in vibration and BVI noise reduction by higher harmonic control, it can be expected to be one of the important ones.

References

- [1] Wood, E.R.; Powers, R.W.; Hammond, C.E.
"On Methods for application of Harmonic Control"
Vertica, Vol. 4, pp. 43-60, 1980.
- [2] Brooks, T.F.; Booth, E.R.
"Rotor Blade Vortex Interaction Noise Reduction and Vibration using Higher Harmonic Control"
16th European Rotorcraft Forum, Glasgow, Scotland, 1990
- [3] Polychroniadis, M.
"Generalized Higher Harmonic Control, Ten Years of Aerospatiale Experience"
16th European Rotorcraft Forum, Glasgow, Scotland, 1990
- [4] Splettstoesser, W.R. et al
"BVI Impulsive Noise Reduction by Higher Harmonic Pitch Control:
Results of a Scaled Model Rotor Experiment in the DNW"
17th European Rotorcraft Forum, Berlin, Germany, 1991
- [5] Kube, R.; Achache, M. Niesl, G.; Splettstoesser, W.R.
"A Closed Loop Controller for BVI Impulsive Noise Reduction by Higher Harmonic Control"
48th Annual Forum of the American Helicopter Society, Washington, DC, 1992
- [6] van der Wall, B.G.
"An Analytical Model of Unsteady Profile Aerodynamics and Its Application to a Rotor Simulation Program"
15th European Rotorcraft Forum, Amsterdam, The Netherlands, 1989
- [7] Schultz, K.-J.; Splettstoesser, W.R.
"Prediction of Helicopter Rotor Impulsive Noise Using Measured Blade Pressures"
43rd Annual Forum of the American Helicopter Society, St. Louis, 1987
- [8] Bramwell, A.R.S.
"Helicopter Dynamics"
Edward Arnold (Publishers) Ltd., London 1976

- [9] Brooks, T.F.
"HHC Study in the DNW to Reduce BVI Noise - An Analysis"
AHS/RAeS International Technical Specialists Meeting - Rotorcraft Acoustics
and Fluid Dynamics, Philadelphia, PA, 1991
- [10] Kube, R.
"New Aspects of Higher Harmonic Control at a Four Bladed Hingeless Model
Rotor"
15th European Rotorcraft Forum, Amsterdam, The Netherlands, 1989
- [11] Splettstoesser, W.R. et al
"BVI Impulsive Noise Reduction by Higher Harmonic Pitch Control: Results of
a Scaled Model Rotor Experiment in the DNW"
17th European Rotorcraft Forum, Berlin, Germany, 1991
- [12] Wall v.d., B.
"The Impact of Rotor Angle of Attack on BVI Noise Trajectories and Rotor
Loading Characteristics"
20th European Rotorcraft Forum, Amsterdam, The Netherlands, 1994
- [13] Mangler, K.W.
"Calculation of Induced Velocities of a Rotor"
Rep. No. Aero. 2247, RAE, Farnborough, Great Britain, Feb. 1948
- [14] Beddoes, T.S.
"A Wake Model for High Resolution Airloads"
International Conference on Rotorcraft Basic Research, Research Triangle
Park, NC, USA, 1985
- [15] Leiss, U.
"Semi-Empirical Simulation of Steady and Unsteady Blade Aerodynamic
Loading"
International Conference on Rotorcraft Basic Research, Research Triangle
Park, NC, USA, 1985
- [16] Bisplinghoff, R.L.; Ashley, H.; Halfmann, R.L.
"Aeroelasticity"
Addison-Wesley Publishing Company, Inc., Reading, Massachusetts, 1957

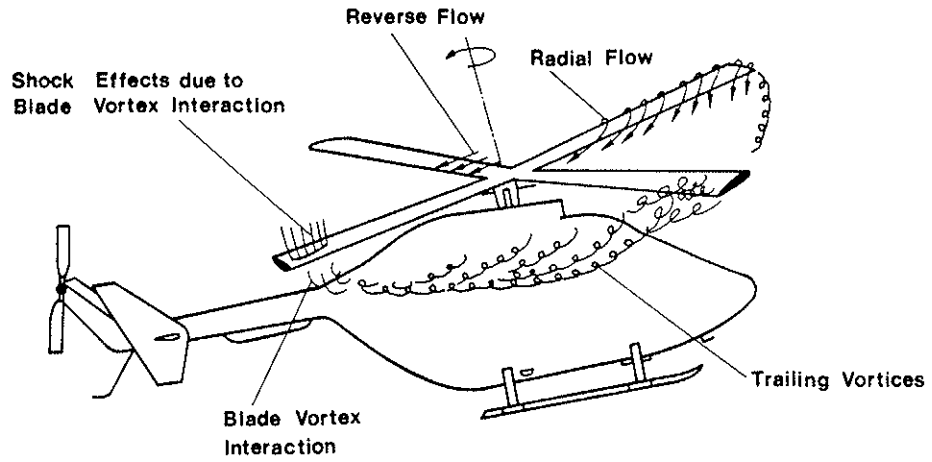


Fig. 1 Aerodynamic Effects in Landing Approach

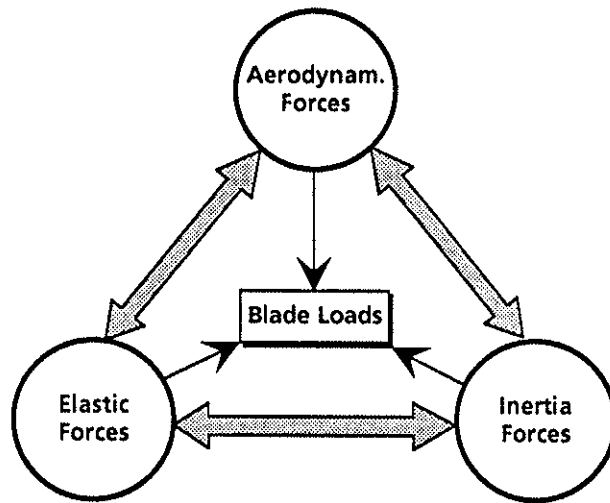


Fig. 2 Rotordynamic Triangle

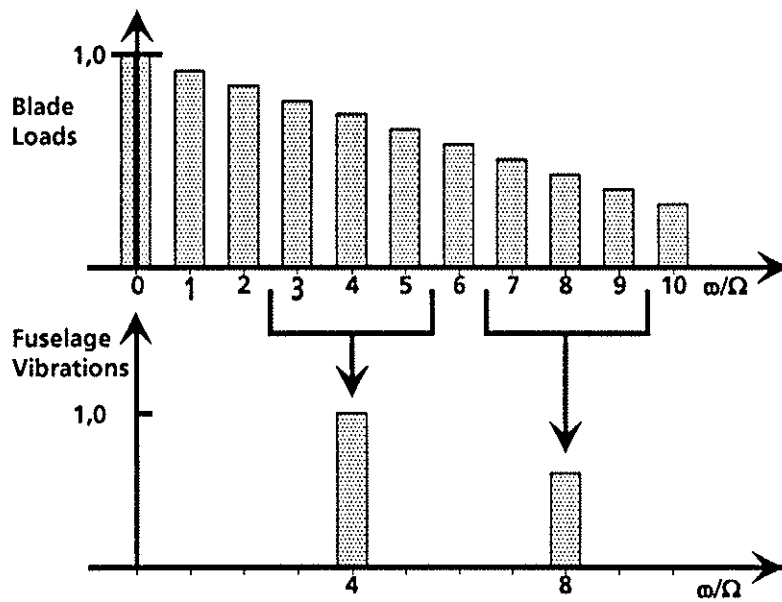


Fig. 3 Vibration Characteristics

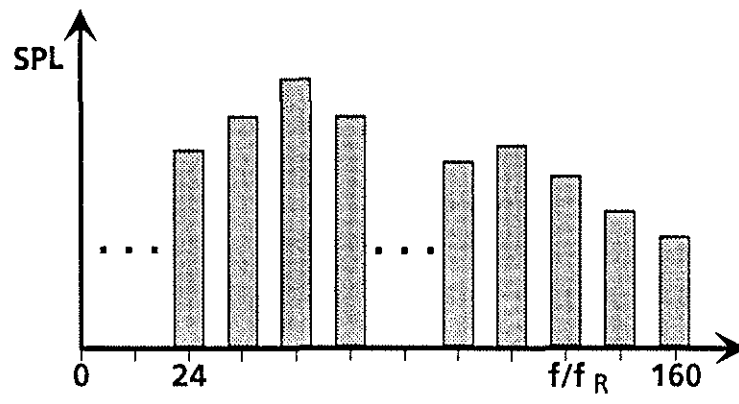


Fig. 4 BVI Noise Characteristics

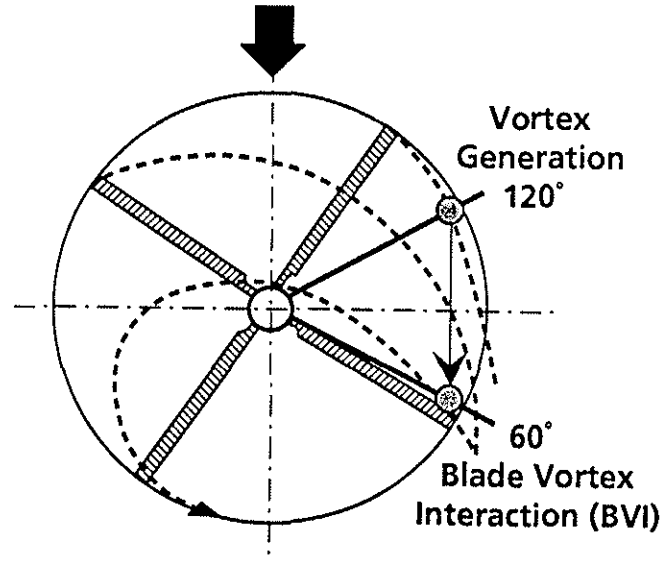


Fig. 5 Vortex Generation and Blad-Vortex Interaction

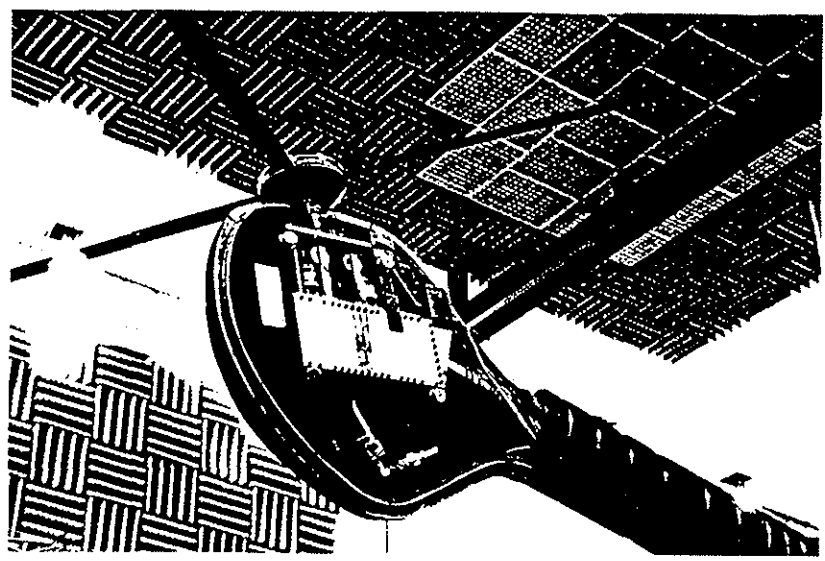


Fig. 6 DLR Rotor Test Rig

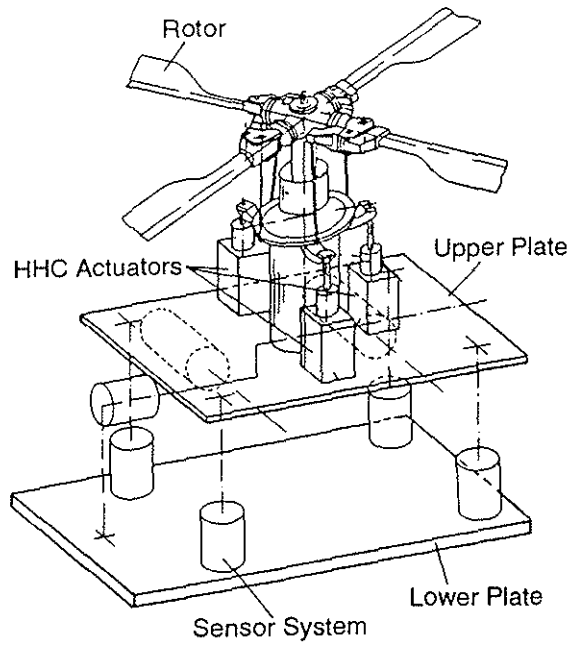


Fig. 7 Rotor Balance

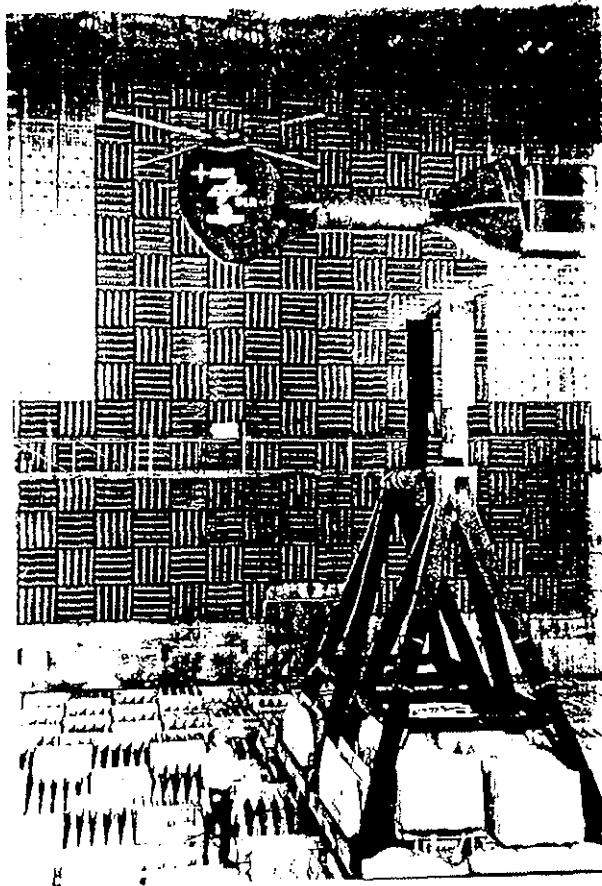


Fig. 8 HHC Test Setup

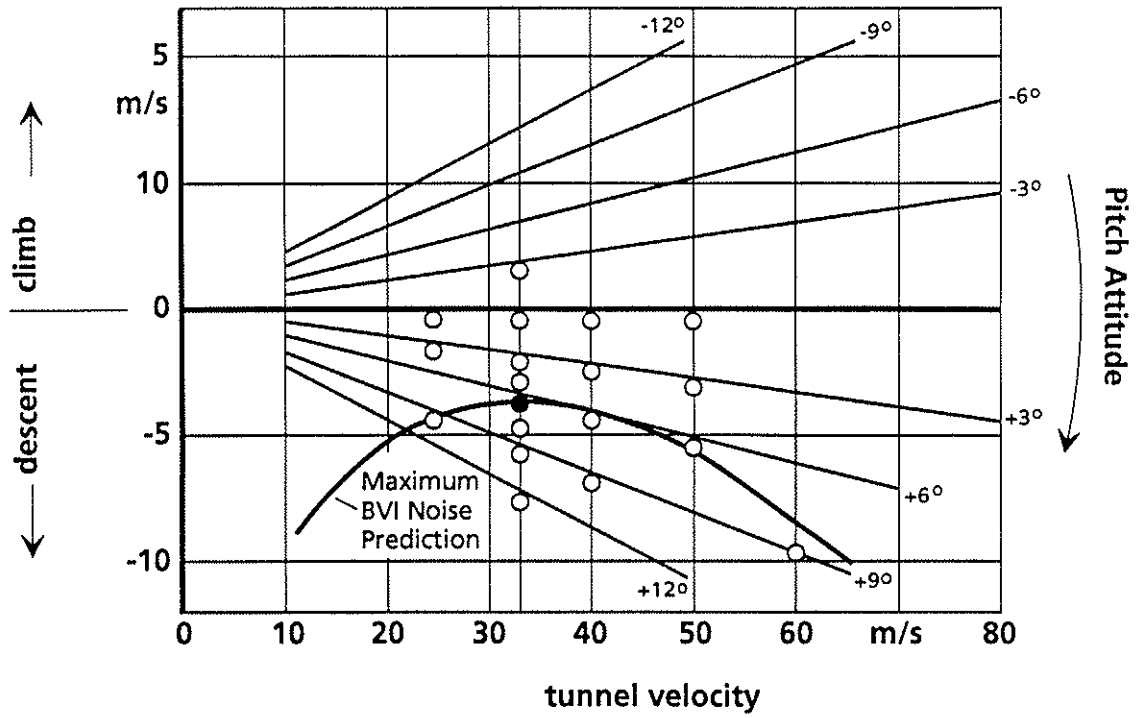


Fig. 9 Wind Tunnel Test Conditions

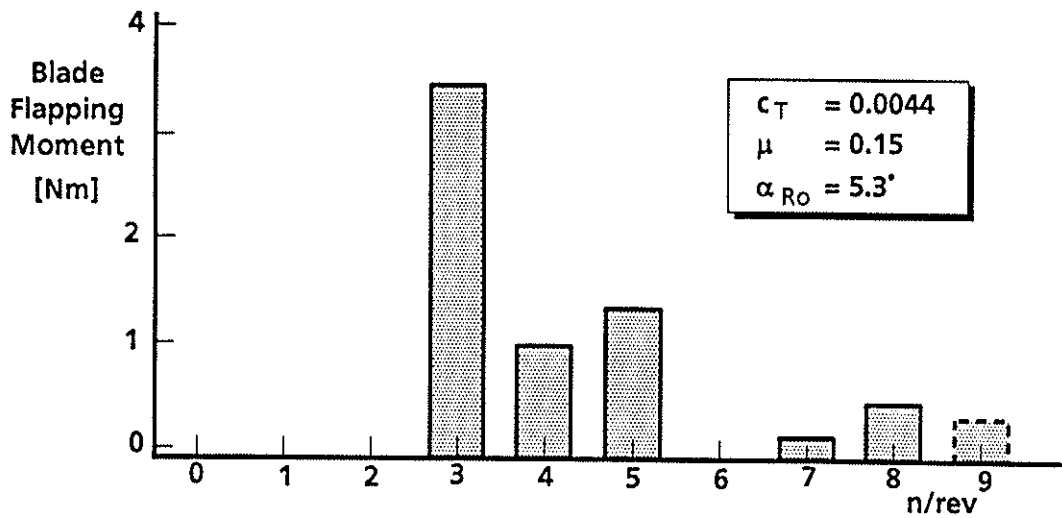


Fig. 10 Vibration Relevant Harmonics of Blade Flapping Moment at $r/R = 0.15$

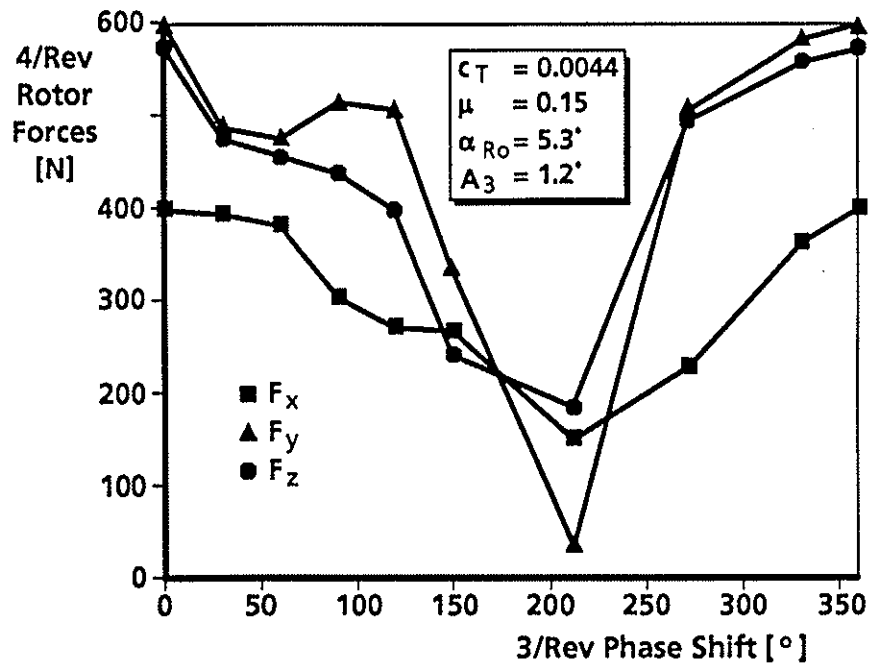


Fig. 11 Dependence of 4/rev Rotor Forces on 3/rev Phase Shift

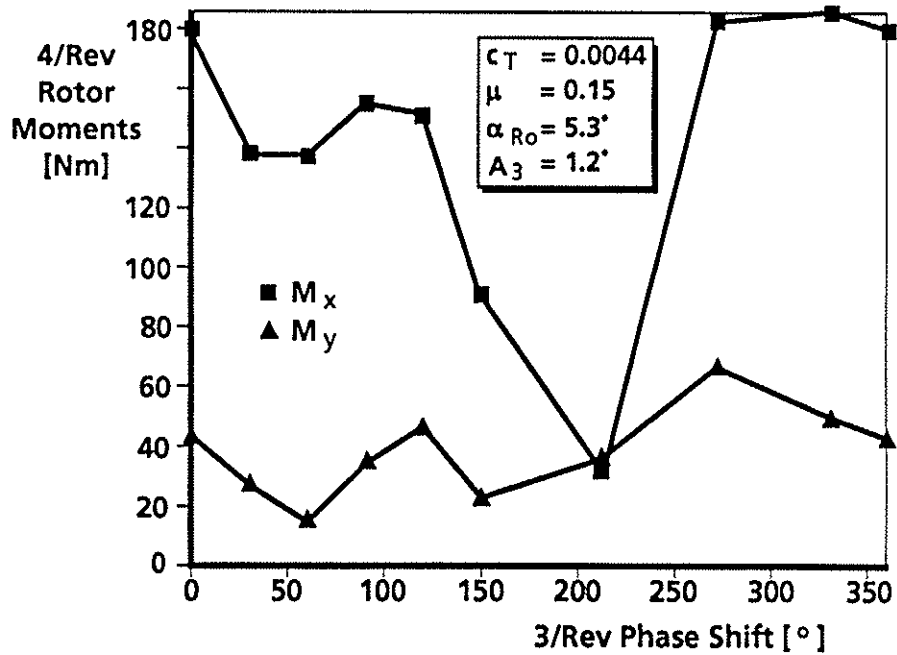


Fig. 12 Dependence of 4/rev Rotor Moments on 3/rev Phase Shift

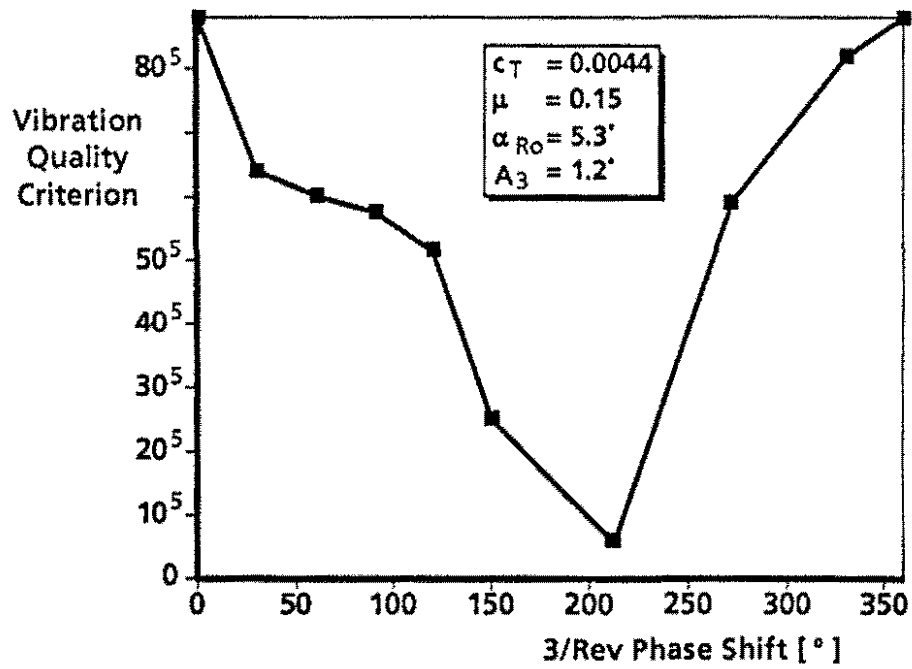


Fig. 13 Dependence of Vibration Quality Criterion on 3/rev Phase Shift

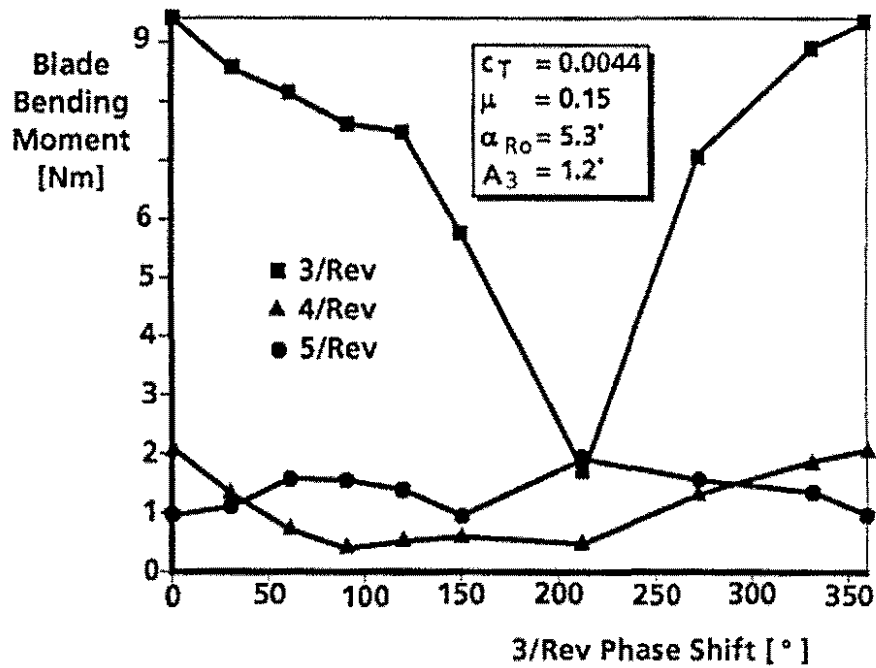


Fig. 14 Dependence of Blade Flap Bending Moment on 3/rev Phase Shift

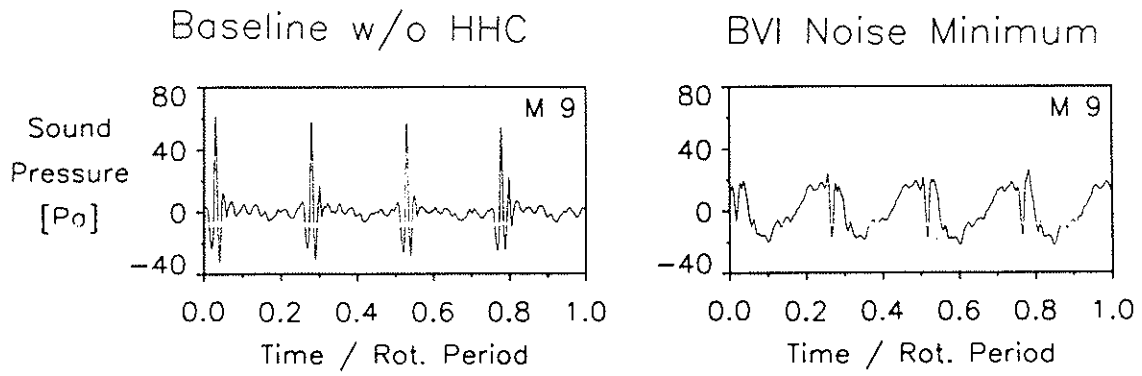


Fig. 15 Sound Pressure Time Histories without and with HHC

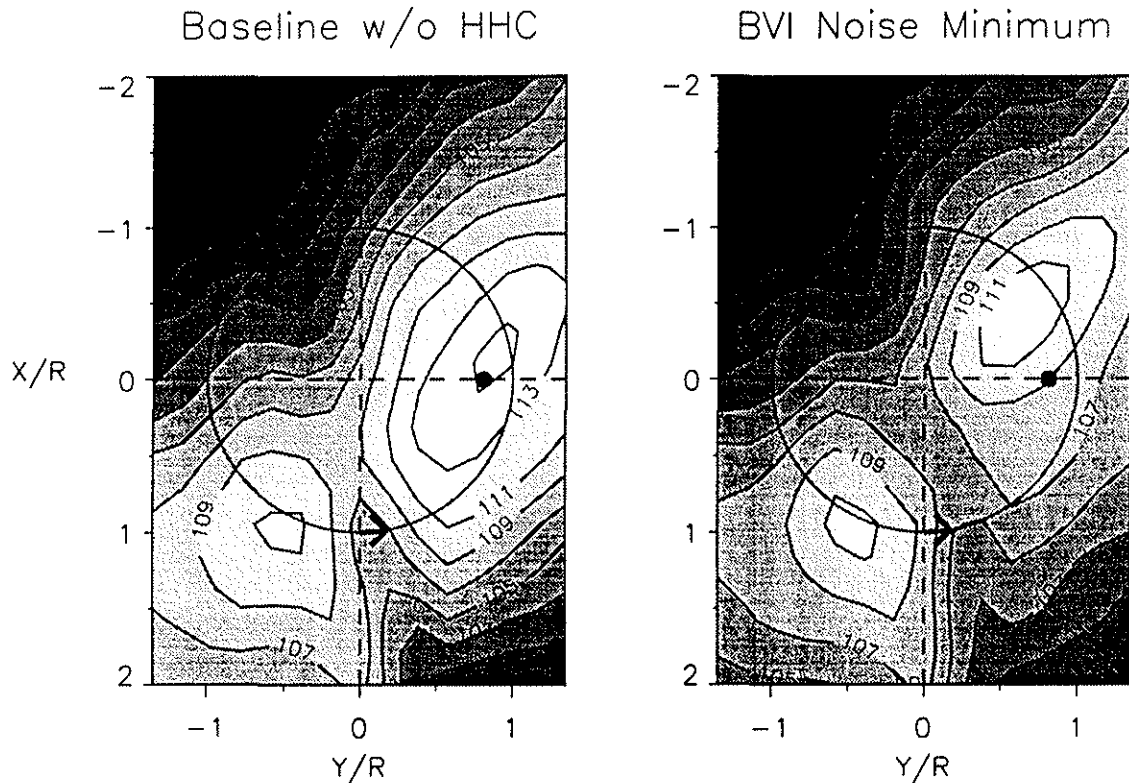


Fig. 16 BVI Noise Pattern Variation with HHC

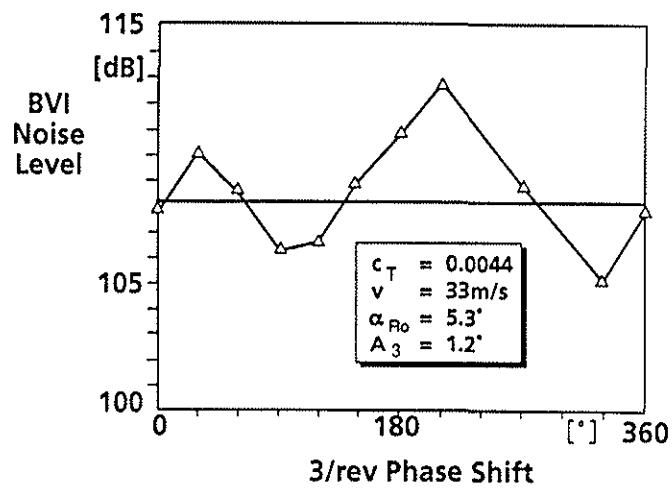


Fig. 17 Dependence of BVI Noise Level on 3/rev Phase Shift

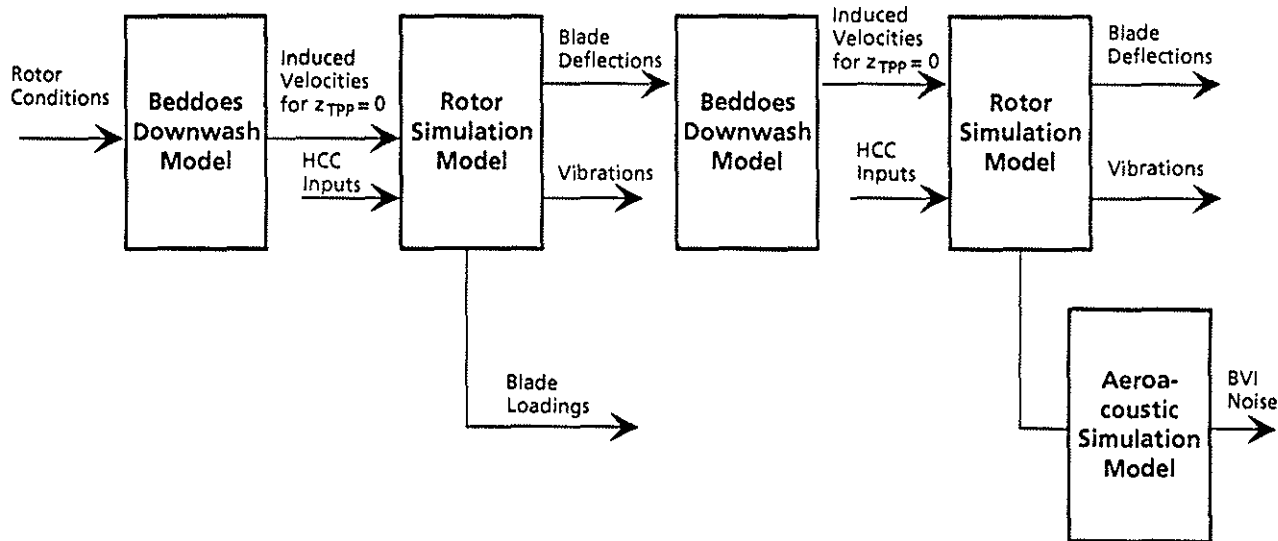


Fig. 18 Simulation Procedure

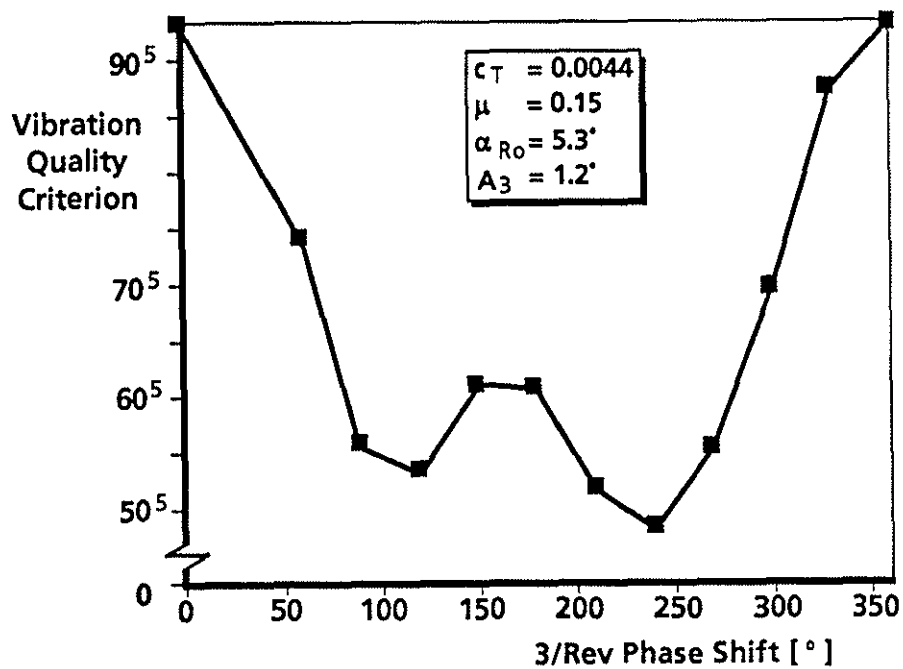


Fig. 19 Simulated Vibration Quality Criterion

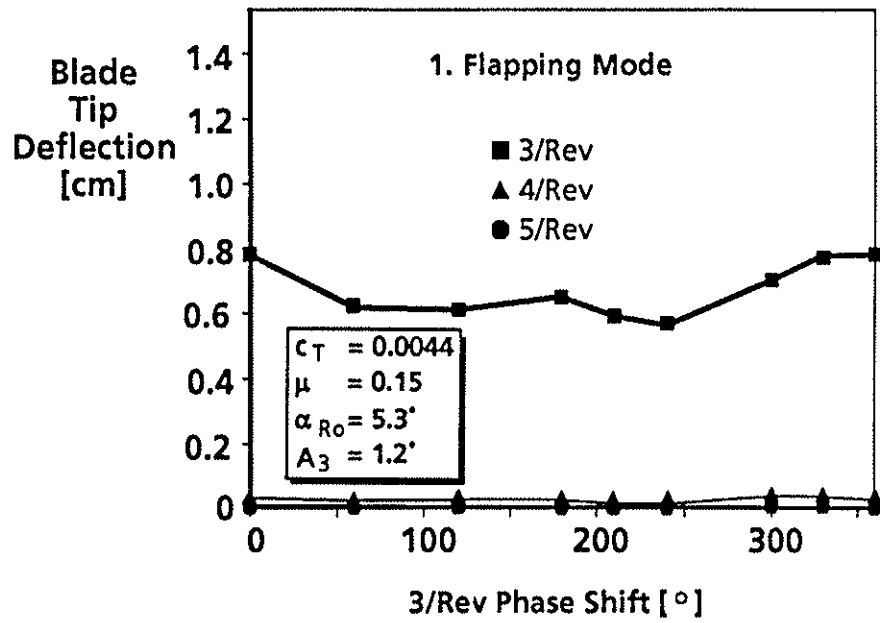


Fig. 20 Variation of 1. Flapping Mode with 3/rev Phase Shift

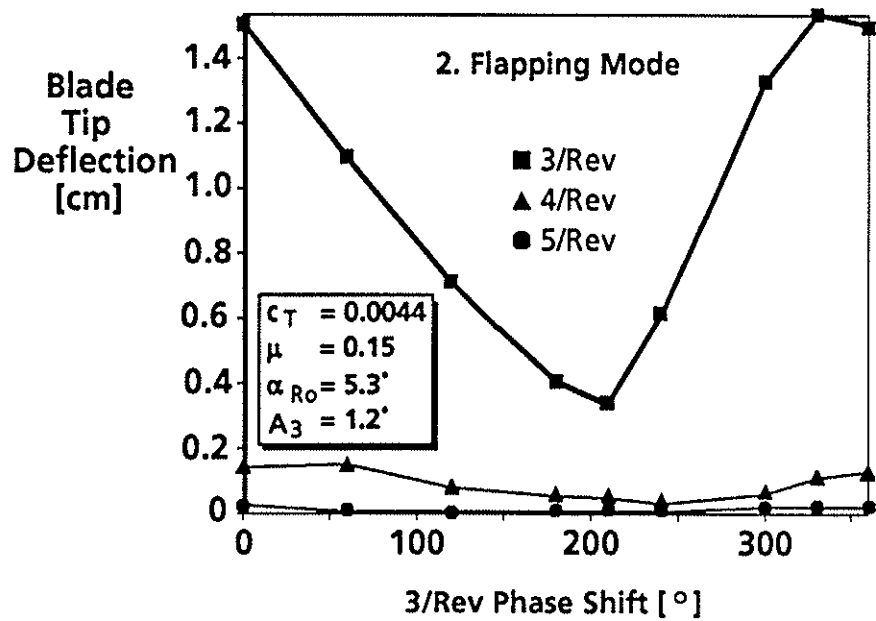


Fig. 21 Variation of 2. Flapping Mode with 3/rev Phase Shift

Blade-Vortex Missdistance/Chordlength

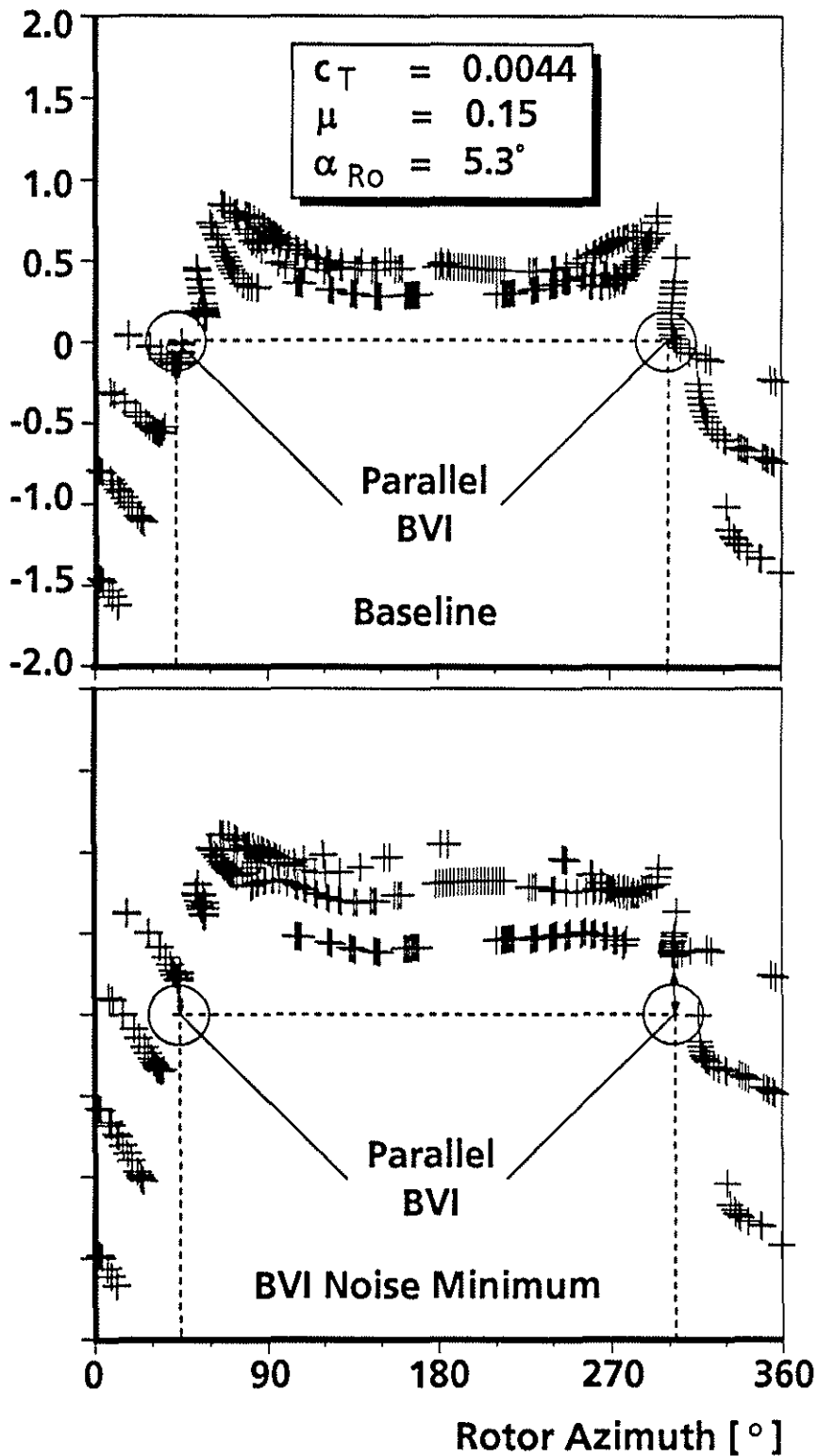


Fig. 25 Simulated Blade-Vortex Missdistance without and with HHC

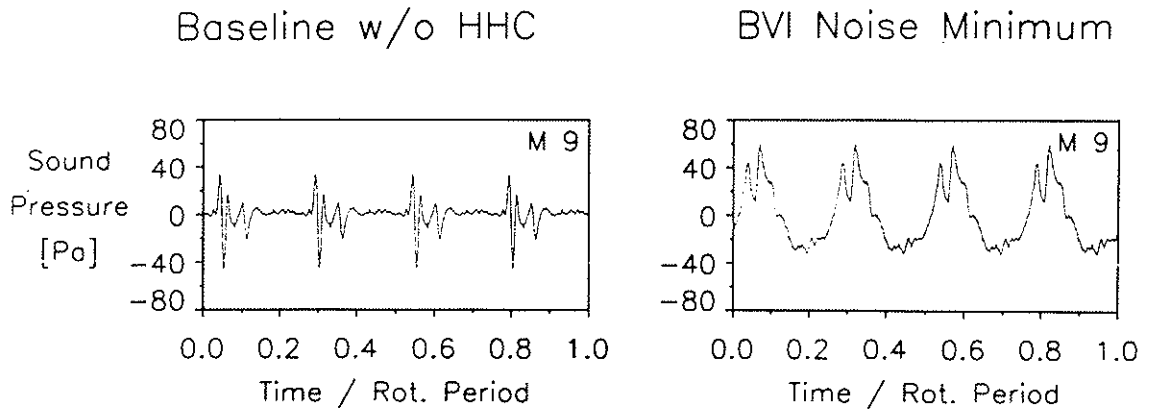


Fig. 22 Sound Pressure Time Histories without and with HHC

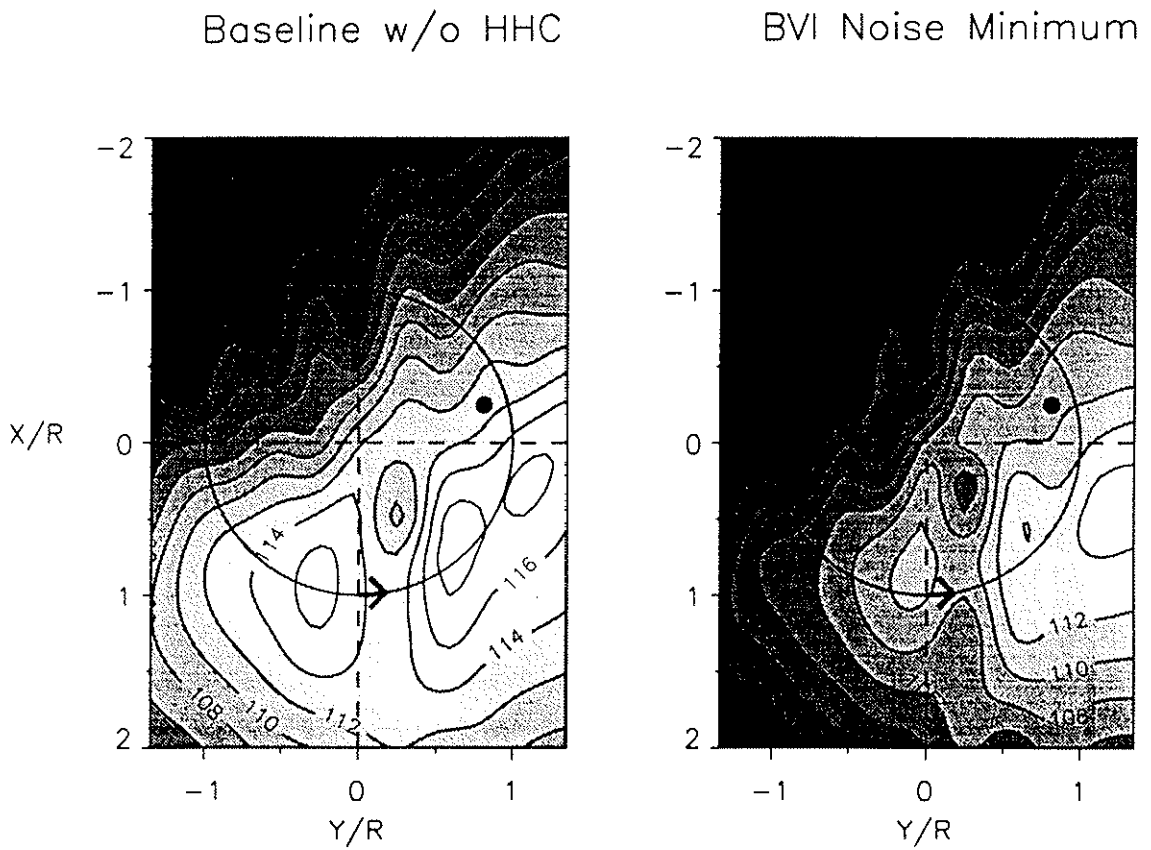
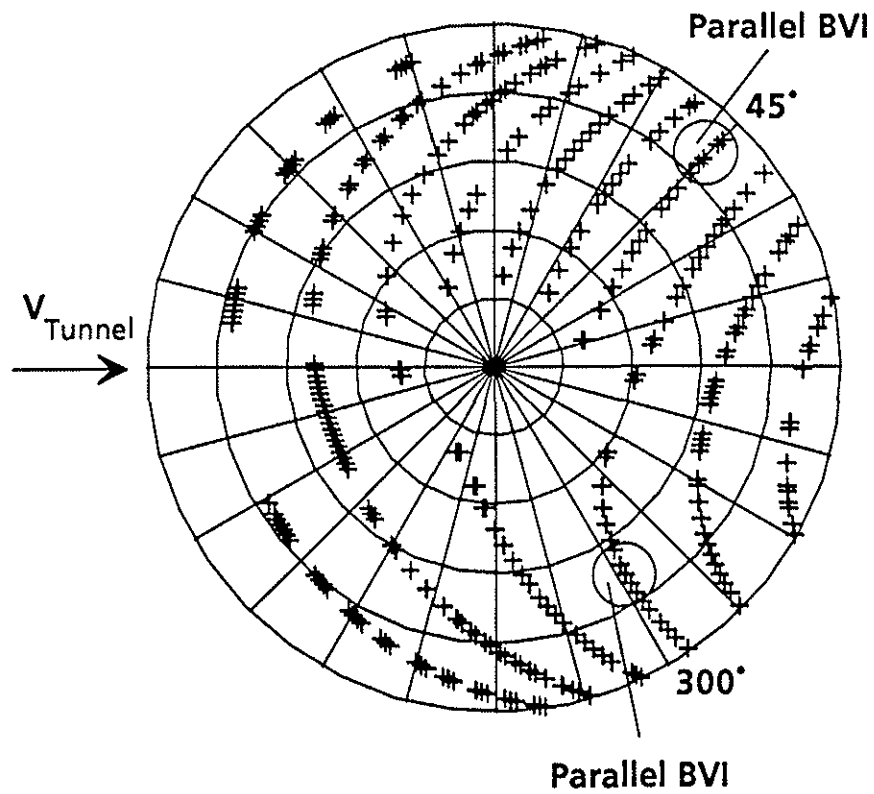


Fig. 23 BVI Noise Pattern Variation with HHC



Blade-Vortex Missdistance/Chordlength

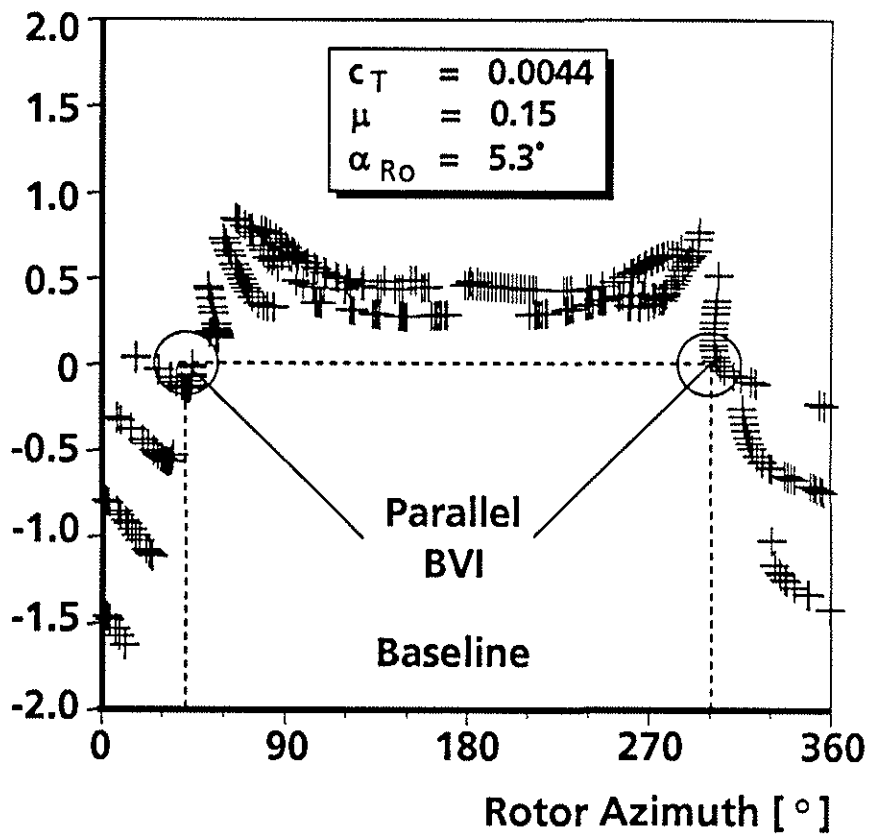


Fig. 24 Simulated Vortex Trajectories and Blade-Vortex Missdistance without HHC

Blade-Vortex Missdistance/Chordlength

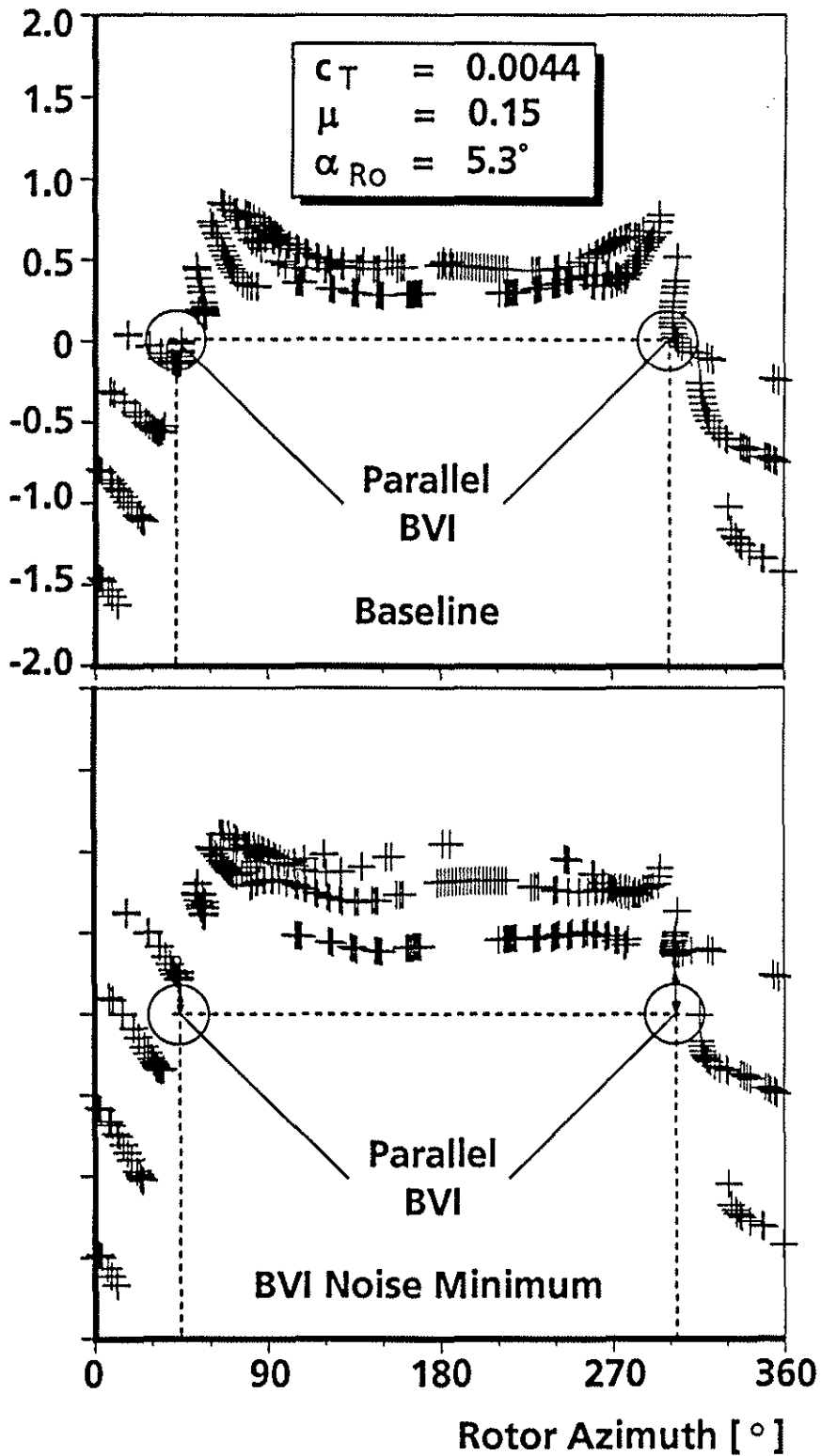


Fig. 25 Simulated Blade-Vortex Missdistance without and with HHC